

Pilot Pattern Design for PUSC MIMO WiMAX-like Filter Banks Multicarrier System

Faouzi Bader and Musbah Shaat

Centre Tecnològic de Telecomunicacions de Catalunya-CTTC
PMT, av. Canal Olímpic s/n. 08860 Castelldefels-Barcelona, Spain
Email: {faouzi.bader, mshaat}@cttc.es

Abstract—In this paper, we analyze different designed pilot patterns adapted to the DL-PUSC pilot grid for filter banks multi-carrier (FBMC) system. Different scheme have been proposed (pair of pilots, auxiliary pilot scheme, interference approximation method, and Scattered pilot method) and their performance evaluated and compared when using conventional cyclic prefix orthogonal frequency division multiplexing (CP-OFDM) system. We shown that by applying certain designed patterns especially for filter banks multi-carrier, the bite error rate can outperforms in certain cases that achieved by the CP-OFDM system. The performance evaluations are done in hypothetical WiMAX scenario on which the FBMC system will substitute the CP-OFDM by maintaining as much as possible the physical layer (PHY) compatibilities.

Keywords-WiMAX, Pilot pattern, Filter banks multicarrier system, OQAM, MIMO, pilot pattern.

I. INTRODUCTION

Wireless multicarrier (MC) communication scheme has proven its effectiveness in many of new communication standards (WiMAX, LTE, DVB-S, WiFi, etc.) [1]. This is not a fortuity, as multicarrier schemes offer many advantages as their robustness in frequency selective channels, their simplicity during the equalization and synchronization processes, besides, their high degree of flexibility and scalability in offering best solutions in scarcity radio resource scenarios. One of the most extended multicarrier schemes is the orthogonal frequency division multiplexing (OFDM), which encompass the advantages cited above, besides is one of the schemes always considered and tested in emerging wide band communication standards. A cyclic prefix (CP) is often used in OFDM which acts as a buffer region where delayed information from the previous symbols can be stored. The OFDM receiver has to exclude samples from the cyclic prefix which got corrupted by the previous symbol. The OFDM scheme is actually used in several communication systems as in e.g., WiFi, WiMAX, DVB-S2, and LTE [1].

Filters bank multiple carrier (FBMC) scheme is actually appearing as an alternative scheme to the conventional OFDM scheme, mainly in cognitive based environments [2] [3] [5] [6]. There are several advantages in using the FBMC than the OFDM, and one of them is the proper use of the CP to cope with the channel impulse response

which results in a loss of capacity, which is not the case in FBMC, added requirements for block processing to maintain orthogonality among all the subcarriers. In OFDM systems, the leakage among frequency sub-bands has a serious impact on the performance of the FFT-based spectrum sensing in cognitive radio (CR) environment. Moreover, to combat the leakage problem in OFDM network a very tight and hard implementation for synchronization has to be imposed among the nodes. Another advantage of using the FBMC scheme, is that the subchannels can be optimally designed in the frequency domain to have a desired or specific spectral containment.

Filter bank MC system (FBMC) with offset quadrature amplitude modulation (OQAM) (named also OQAM-OFDM) can achieve smaller intersymbol interference (ISI) and intercarrier interference (ICI) without using the CP, by using well designed pulse shapes that satisfy the perfect reconstruction conditions. Moreover, the problem of the spectral leakage can be solved by minimizing the side-lobes of each subcarrier which leads to high efficiency (in terms of spectrum and interference) [4]-[7].

So far, some attempts have been made to introduce the FBMC in the radio communications arena, through proprietary schemes, in particular the IOTA technique (see: TIA-902.BBAB, Wideband air interface Isotropic Orthogonal Transform Algorithm (IOTA) physical layer specification, document of the Telecommunications Industry Association [8] [9], and in 3GPP TSG-RAN WG1. TR25.892, Feasibility study of OFDM for UTRAN enhancement. V1.1.0, June 2004). However, the full exploitation of FBMC techniques and their optimization in the context of radio evolution, such as dynamic access, as well as their combination with MIMO techniques, have not been considered. Physical Layer for Dynamic Spectrum Access (PHYDYAS) FP7 European project with code ICT-211887 [2], is one of the pioneer research projects at the European level that tried to resolve pending technical challenges for a real exploitation of the FBMC scheme.

In this paper, the authors present a FBMC system that aims to maintain a certain degree of compatibility with

the OFDM based WiMAX specifications described in IEEE 802.16e standard [11]. Several pilot patterns for channel estimation are here proposed and analyzed for FBMC following the MIMO downlink (DL) partial usage of subcarriers (PUSC) frame structure of WiMAX, but due to the nature of the FBMC system, the pilots cannot be as straightforwardly applied as in OFDM. The main reason is that, every FBMC pilot symbol besides suffering the traditional effect of the additive white Gaussian noise (AWGN) a new interference component from frequency-time surrounding subchannels is added, what will affect the well acquisition of the pilot information at the receiver, therefore, results a degradation on the system capacity.

This paper is an extension of the analysis presented by the authors in [10], where the pilot pattern adaptation for FBMC included only the interference "approximation method" (IAM) and the "auxiliary pilot" scheme for channel estimation. In this paper, besides results presented in [10], the authors proposed new pilot patterns as the "pair of pilots" and the "scattered pilots" methods. Note that, the added pilot schemes are always designed considering the specificity of the FBMC scheme and the mitigation of the surrounding interference effect.

The paper is structured as follow: a brief overview on pilot allocation structures in WiMAX system is presented in Section II. The structure of the FBMC communication system and its adaption to the downlink partial usage of subcarriers (PUSC) specifications using MIMO with different proposed pilot patterns structures are presented in Section III. Section IV, introduces the simulation setup, and presents achieved performances. Finally, in Section V, the main conclusions on obtained results are drawn.

II. BRIEF OVERVIEW OF PILOT ALLOCATION STRUCTURES IN WiMAX SYSTEMS

The general statement and frame structure of WiMAX system for the time division duplex (TDD) mode can be found in [11]. To ensure the compatibility of FBMC system with WiMAX (at least within the context of pilot allocation) these statements have to be considered as basis within the ICT-PHYDYAS project [2] [3]. WiMAX offers three different subcarrier permutation schemes [11]. The first, is the Full Usage of the Subchannels (FUSC) scheme allocates first the pilots on fixed positions, and the remaining subcarriers are used to transmit the data. The second and the third schemes are the Partial Usage of the Subcarriers (PUSC), and the Band Adaptive Modulation and Coding schemes (later referred as AMC) respectively, which divide the whole frame (excluding the Preamble, the PCH and DL/UL-MAPs) into minimal data units (named slots), where dedicated pilots and data are jointly allocated. Each slot is defined as a two dimensional units which spans in both frequency and time

directions.

A. Pilot and data allocation for the PUSC, AMC and FUSC modes

1) *PUSC mode*: The shape of one slot in the PUSC scheme is two clusters in frequency direction and two OFDM symbols in the time direction. Hence, the number of data subcarriers is 48. Due to subchannel permutation the clusters are transmitted at distant positions in the spectrum, although each cluster is transmitted as a whole in adjacent subcarriers. Consequently, the PUSC permutation scheme increases the frequency diversity.

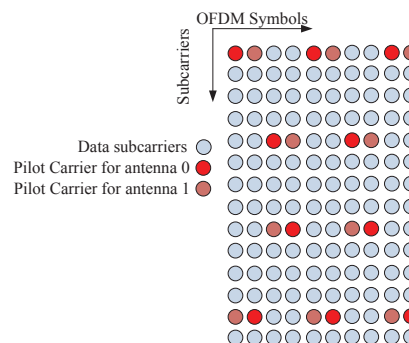


Figure 1. Cluster structure for STC downlink PUSC using 2 antennas.

2) *AMC mode*: The AMC permutation scheme is characterized by mapping adjacent subcarriers to each slot. By doing so, although frequency diversity is minimized. The use of adaptive modulation and coding may lead to great benefits by transmitting for each user on those bands where the channel experiences favorable conditions. For this permutation scheme, a smaller resource unit defined by nine contiguous subcarriers is used. This basic allocation unit is referred to as a 'bin'. Each bin contains one pilot subcarrier (whose position is changed every OFDM symbol) and eight data subcarriers. There are four types of AMC slots. The first is given by the collection of six consecutive bins (hence a 6×1 structure), the second has a 2×3 structure, and the third and the fourth are given by the 3×2 and the 1×6 structures respectively.

3) *FUSC mode*: For the FUSC permutation scheme, the symbol structure is constructed using pilot, data and empty subcarriers. Pilots and empty subcarriers are first allocated. The remaining subcarriers are then used as data subcarriers. 48 data subcarriers are later mapped to each subchannel. The subcarriers from each subchannel is mapped to physical subcarriers and placed equidistantly in the spectrum. For the FUSC scheme, one slot is defined as one subchannel per one OFDM symbol, thus giving a total of 48 data subcarriers. Figure 2, shows an example of the location of the pilots within one cluster for two transmit antennas. It

can be observed that the position of the pilot symbols from the variable set change each two OFDM symbols. Designed pilot patters for FBMC will focus mainly on the downlink PUSC scheme.

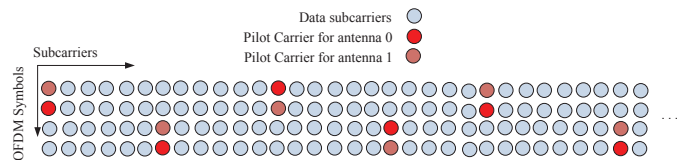


Figure 2. Cluster structure for STC FUSC using 2 antennas.

III. FBMC SCHEME AND PILOT ALLOCATION

The hereafter subsections describe the transmission and reception structures of the FBMC scheme, the specificity operation of allocating pilots within a FBMC frame compared with conventional OFDM, and the different designed pilot pattern schemes considering the specificity of the FBMC.

A. Filter Bank based multicarrier structure

In FBMC, the filters bank are used in the transmultiplexer configuration using the synthesis filter bank (SFB) at the transmitter side, and the analysis filter banks (AFB) at the receiver side [11][12] (see Figure (3)). In FBMC systems, the use of critically sampled filter banks would be problematic, since the aliasing effects would make it difficult to compensate imperfections of the channel by processing the subchannel signals after the AFB only. Therefore, a factor of two oversampling is commonly applied in the subchannel at the AFB (see Figure (3b)).

In this paper the authors focused on uniform modulated filters bank with a prototype filter $g[m]$ of length L which is shifted to cover the whole of the system bandwidth. The output signal from the synthesis filter bank is given by

$$S[m] = \sum_{k=0}^{M-1} \sum_{n \in Z} d_{k,n} g[m-n \frac{M}{2}] e^{j2/Mm(m-\frac{D}{2})} e^{j\varphi_{k,n}} \quad (1)$$

where D is the delay term which depends on the length of the prototype filter $g[m]$, and $\varphi_{k,n}$ is an additional phase term. The transmitted symbols $d_{k,n}$ are real-valued symbols. Equation (1) can be written in a more compact form such that

$$S[m] = \sum_{k=0}^{M-1} \sum_{n \in Z} d_{k_p, n_p} g_{k,n}[m] \quad (2)$$

where M is the number of subcarriers ($M=IFFT/FFT$ size) and also the number of active subcarriers, $d_{k,n}$ denotes the real-valued symbol at the k -th subcarrier during the n -th symbol interval, modulated at rate $2/T$. The signalling interval T is defined as the inverse of the subcarrier spacing, i.e., $T = 1/\Delta f$. The symbols $d_{k,n}$ and $d_{k,n+1}$ can be

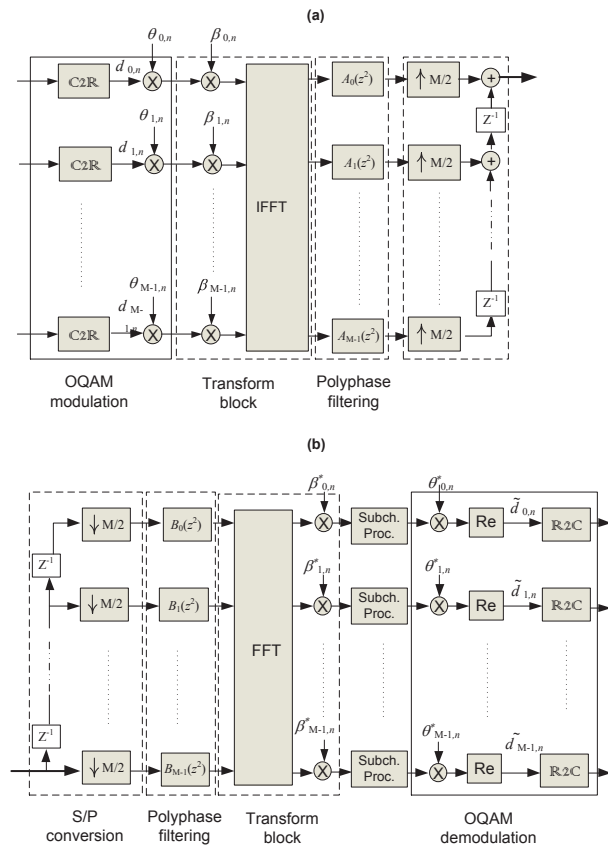


Figure 3. Multicarrier polyphase filter bank for SISO case, (a) Synthesis filter bank, (b) Analysis filter banks.

interpreted as the in phase and quadrature (I/Q) components respectively of the complex-valued symbol $c_{k,l}$ (of rate $1/T$) from a QAM-alphabet. The phase term $\varphi_{k,n}$ in equation (1) guaranty and holds the real orthogonality condition [18] by having,

$$\Re \sum_{m=-\infty}^{+\infty} g_{\hat{k}, \hat{n}}[m] g_{n, \hat{k}}^*[m] = \delta_{k, \hat{k}} \delta_{n, \hat{n}} \quad (3)$$

The synthesized signal burst is therefore a composite of multiple subchannel signals each of which consists of a linear combination of time-shifted (by multiples of $T/2$) and overlapping impulse responses of the prototype filter, weighted by the respective symbol values $d_{k,n}$. L is the length of the filter prototype $p[m]$ and depends on the size of the filter bank and the overlapping factor K by having $L = KM$ [12][13]. The "C2R" and the "R2C" blocks in Figure 3, indicate the conversion of the data from complex into real form, and the inverse operation respectively. Note that each sub-carrier is modulated with an Offset Quadrature Amplitude Modulation (OQAM) which consists in transmitting the real and the imaginary parts of a

complex data symbol with a shift of half the symbol period between them [13] [14].

B. Pilot allocation in FBMC

In FBMC system, either real or imaginary parts of the complex symbols are used for data transmission in a staggered manner. When a real (imaginary) part of a subcarrier symbol is used, the unused imaginary (real) part is at the receiver a fairly complicated function of surrounding data symbols. Usually in OFDM systems recovering the channel state information (CSI) is first proceed from known time and frequency pilot locations within certain intervals. The whole signal is recovered by means of different interpolation techniques [15]. Therefore, the channel state information (CSI) recovery process in OFDM is simple. However, this is not the case in filters bank systems, here every FBMC time-frequency pilot position is contaminated or suffered interference from the neighboring subchannels (see descriptive scheme in Figure 4) [16]. With ideal channel this interference is only located on the imaginary part of the subchannel signal. Thus, the real part yields the originally transmitted symbol $d_{k,n}$. Note that this interference depends on the real (imaginary) data around the pilot frequency-time position (k, n) , and has a random variable behavior sometime close to zero. Therefore, sending a known symbol at a known time-frequency location is not enough, since at the receiver side the interference part will depends on the surrounding data [2] [16] values.

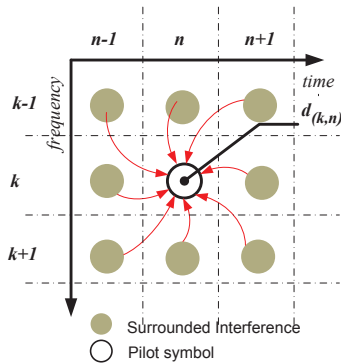


Figure 4. Time-frequency pilot location in a FBMC system with surrounded interferes.

The contribution weights on the interference of the data surrounding a certain symbol closely coincide with the response of the filter banks and depend on the design of the prototype filter. Table I, shows the filter banks weights used in this paper [2] [14] [18]. As a resume, the nature of FBMC systems makes it impossible to construct pilot symbols for channel estimation in the same way as in OFDM.

Table I
REPRESENTATION OF THE TIME-FREQUENCY RESPONSE OF THE FBMC SYSTEM CONSIDERED IN THIS WORK. DUE TO THE EMPLOYED OFFSET QAM MODULATION, THE EFFECTIVE TIME-FREQUENCY RESPONSE WILL BE REDUCED TO ONLY BOLD VALUES IN [2].

| | | | | | | |
|-----------|--------|-----------------|---------------|-----------------|---------|--------|
| 0.0006 | 0.0001 | 0 | 0 | 0 | 0.0001 | 0.0006 |
| -j0.00429 | 0.1250 | j 0.2058 | 0.2393 | j 0.2058 | 0.1250 | j0.049 |
| -j0.0668 | 0.0002 | 0.5644 | 1.000 | 0.5644 | 0.0002. | 0.0668 |
| j0.00429 | 0.1250 | j 0.2058 | 0.2393 | j 0.2058 | 0.1250 | j0.049 |
| 0.0006 | 0.0001 | 0 | 0 | 0 | 0.0001 | 0.0006 |

C. Pilot pattern adaptation for FBMC downlink PUSC scheme: the MIMO context

Using the PUSC permutation, the set of active subcarriers is divided into clusters. The Pilots and the data subcarriers are allocated within each cluster [11], each one formed by 14 adjacent carriers, where two of them are dedicated to pilot symbols. In case of single antenna transmission, the pilots' positions are changing between each odd and even symbols. In case of two transmitting antennas, the pilots are placed following the scheme in Figure 5a. Specific pilot locations are reserved and exclusively used by each antenna. A proposed pilot pattern for a 2×2 FBMC system is shown in Figure 5b. This structure is built considering a time oversampling equal to $T/2$. That means that the relative pilot overhead using this structure is the same as that considering an OFDM system, i.e., for each pilot one offset quadrature amplitude modulation is used in FBMC. Therefore, one QAM symbol will be used in OFDM. At the AFB side, the received output signal samples of the interest pilot symbol at the frequency-time position (k_p, n_p) can be expressed as:

$$r_{k_p, n_p} \simeq h_{k_p, n_p}(d_{k_p, n_p} + j t_{k_p, n_p}) + z_{k_p, n_p} \quad (4)$$

where h_{k_p, n_p} and z_{k_p, n_p} are the channel coefficient and the noise term respectively at pilot subcarrier k_p and time index n_p . According to the values depicted in Table I, we note that most part of the energy is localized in a restricted set (shown in bold) around the considered symbol. Consequently, we assumed in (4) that the intrinsic interference term depends only on this restricted set (denoted by (k, n) in (5)). Moreover, we assume that the channel is quasi-static at least over all this zone. The value $t_{k, n}$ is defined as an intrinsic interference and is equal to,

$$t_{k_p, n_p} = \sum_{(k, n) \neq (k_p, n_p)} h_{k_p, n_p} d_{k, n} \sum_{m=-\infty}^{+\infty} g_{k, n}[m] g_{n_p, k_p}^*[m] \quad (5)$$

In case having a MIMO system with N_t transmit antennas and N_r receive antennas, the real (imaginary) pilot symbol $d_{k, n}^{(i)}$ is transmitted at the frequency-time position $(k_p; n_p)$ over the transmit antenna i ($i \in \{1, \dots, N_t\}$). So, after transmitting through the radio channel, we demodulated at

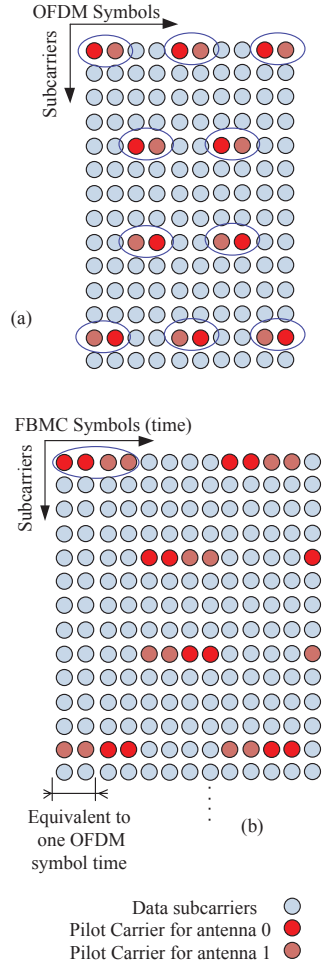


Figure 5. Pilot pattern for 2×2 antennas, (a) cluster structure for STC downlink PUSC in WiMAX, (b) STC PUSC adapted to FBMC.

the j -th received antenna [17], and the received signal is,

$$r_{k_p, n_p}^{(j)} = \sum_{i=1}^{N_t} h_{k_p, n_p}^{(j, i)} (d_{k_p, n_p}^{(i)} + j t_{k_p, n_p}^{(i)}) + z_{k_p, n_p}^{(j)} \quad (6)$$

where $h_{k_p, n_p}^{(j, i)}$ is the channel coefficient between transmit antenna "i" and receive antenna "j". If the prototype filter is designed with good frequency selectivity and a roll-off factor $\alpha \leq 1$, the range includes k_p with both adjacent subcarriers $(k_p - 1)$ and $(k_p + 1)$ in the frequency direction.

D. FBMC adaptation using auxiliary pilot scheme

C. L  l   et al. used in [18] the "auxiliary pilot" concept in OQAM-OFDM preamble for channel estimation. This concept, was in this paper used and adapted to deal with the channel estimation process in a FBMC MIMO system. In Figure 6, a modified scheme from that depicted in Figure 5b

is presented to use auxiliary pilot scheme in a MIMO-FBMC system. As it can be shown in Figure 6, two types of pilots per antenna are used, each one allocated in a predefined position within the FBMC frame. As described in [2] [3] and [19], the main goal of the auxiliary pilot (named also as 'help pilot') position located adjacently to the pilot position (k_a, n_a) is to cancel the extra interference effect appeared in (5).

In other words, the interference part that affects the pilot must become equal zero, or small enough to be neglected. The main reason by introducing a spacing between both pair of pilots (one per each antenna) in Figure 6, is to avoid to have an auxiliary pilot in the window of another auxiliary pilot as recursive calculation of auxiliary pilots would be required (see the filter weights values in Table I), which may be somewhat inconvenient. However, using this slightly modified pilot pattern scheme this difficulty can be avoided, and each of the auxiliary pilots can be calculated independently. For MIMO case, this can be achieved by choosing the value of the auxiliary pilot equal to

$$d_{k_a, n_a}^i = \frac{\sum_{(k, n) \in \Omega_{k_p, n_p} \atop (k, n) \neq (k_p, n_p) \atop (k, n) \neq (k_a, n_a)} d_{k, n}^i \hat{u}_{k - k_p, n - n_p}}{\hat{u}_{k_p - k_a, n_p - n_a}} \quad (7)$$

Note that it is preferable to choose the auxiliary pilot in such a way that the magnitude of the denominator is maximized.

E. FBMC using Interference Approximation Method (IAM)

The interference approximation method (IAM) was presented by C. Lele et al. in [18] for preamble-based channel estimation using the Isotropic Orthogonal Transform Algorithm (IOTA) scheme [9].

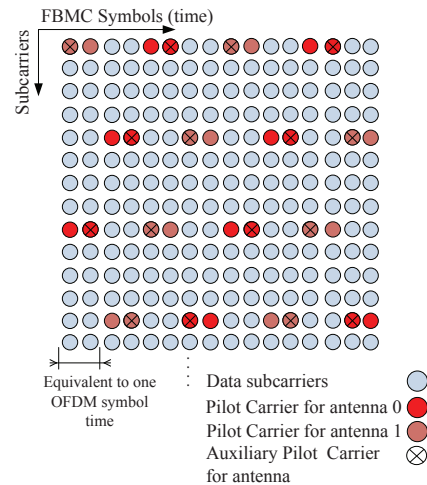


Figure 6. Pilot and auxiliary pilot pattern structure for 2×2 MIMO FBMC system.

The method is based on the assumption that the contributions come only from the first frequency-time order neighboring positions. The authors, extended this concept to the MIMO mode using two antennas at the transmitter. The pilot pattern structures proposed is depicted in Figure 7. In Figure 7a, a set of three pilot positions are reserved for each antenna i . The pilot symbol d_{k_p, n_p}^i is first located in the center position of this set, the remained pilots $d_{k_p, n_{p-1}}^i$ and $d_{k_p, n_{p+1}}^i$ are here named as "Aided Pilot Carrier" (APC), as their main function is to aid the pilot d_{k_p, n_p}^i to obtain an approximation of the interference generated by the filter banks. Note that, in both depicted structures in Figure 7 (7a, and 7b), we dealt with partial interference as the amount of interference of Ω_{k_p, n_p} that affects the pilot d_{k_p, n_p}^i could not be here estimated. In Figure 7b, we confined with the information from the $(k_p, n_p - 1)$, $(k_p, n_p + 1)$, $(k_p - 1, n_p)$, and $(k_p + 1, n_p)$ APCs frequency-time positions. We focused on the case where the pilots' positions $(k_p, n_p - 1)$, $(k_p, n_p + 1)$ of each antenna are forced to zero. Therefore, forcing the largest interference weights caused by the filter bank contributions (see values in Table I) (i. e., $|u_{k, n+1}| = |u_{k, n-1}| = 0.5644$) to zero. The interference weight at the frequency-time positions $(k_p - 1, n_p)$, and $(k_p + 1, n_p)$ is $|u_{k-1, n}| = |u_{k+1, n}| = 0.2393$, which have relatively lowest interference weights. This approach allows to maximize the modulus of the resulting pilot, and hence to minimize the noise effect.

F. FBMC using pair of pilots (POP) scheme

As previously mentioned, in FBMC the channel estimation issues is different of that in conventional cyclic prefix OFDM. The reason is that, as already point out, the sought channel frequency response values are complex whereas the training input is real. Moreover, the AFB output samples also contain imaginary contributions from neighboring times and frequencies directions. Under the assumption of having a good time-frequency localization with the employed filter prototype, and a relatively low channel frequency selectivity, J. P. Javaudin et al. proposed in [19] the POP method for coming up with the channel acquisition in a QAM-OFDM system using two preamble symbols. The authors modified proposed POP scheme in [19] to deal with channel estimation in a MIMO FBMC system using modified PUSC pilot pattern scheme depicted in Figure 5b. Here the pairs of pilots relies on simple algebraic relations for the input/output samples in two time slots, and aims at computing a channel estimate operation by using (4) in two different (in practice consecutive) time slots $\{n, n + 1\}$ to construct a system of equations using the real and imaginary parts of a channel gain $H_{k, n}^{(c)}$ (c , means complex value). Note that $H_{k, n}^{(c)} = H_{k, n}^R + jH_{k, n}^I$ R and I refer to the "Real" and "Imaginary" parts. The pilot pattern proposed in Figure 5b, preserves the orthogonality between each antenna's pilots. To describe the POP's channel information acquisition, we denote by

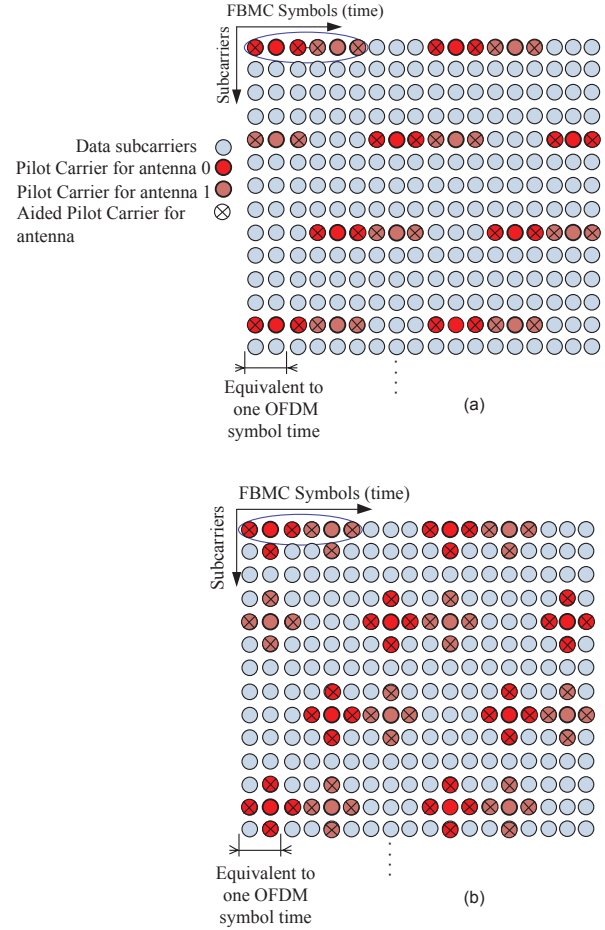


Figure 7. Pilot and pilot support using IAM concept for FBMC in DL-PUSC mode for 2 antennas: (a) reserved allocation for pilots, (b) pilot and aided pilot carrier (APC) positions.

(k_p, n_p) and (k_p, n_{p+1}) the frequency-time positions of the two pilots d_{k_p, n_p}^i and $d_{k_p, n_{p+1}}^i$ respectively (i refers to the antenna index). The value $W_{k_p, n_p}^{(c)} = \frac{1}{H_{k_p, n_p}^{(c)}}$ correspond to the zero forcing (ZF) equalization coefficient. By neglecting the noise part in (4), once can have for each even k a received signal at the j -th antenna as,

$$\begin{cases} r_{k_p, n_p}^{(j)} W_{k_p, n_p}^{(j, i)} = d_{k_p, n_p}^{(i)} + j t_{k_p, n_p}^{(i)} \\ r_{k_p, n_{p+1}}^{(j)} W_{k_p, n_{p+1}}^{(j, i)} = d_{k_p, n_{p+1}}^{(i)} + j t_{k_p, n_{p+1}}^{(i)} \end{cases} \quad (8)$$

Then

$$\begin{cases} r_{k_p, n_p}^{R, (j)} W_{k_p, n_p}^{R, (j, i)} - r_{k_p, n_p}^{I, (j)} W_{k_p, n_p}^{I, (j, i)} = d_{k_p, n_p}^{(i)} \\ r_{k_p, n_p}^{I, (j)} W_{k_p, n_p}^{R, (j, i)} + r_{k_p, n_p}^{R, (j)} W_{k_p, n_p}^{I, (j, i)} = d_{k_p, n_{p+1}}^{(i)} \end{cases} \quad (9)$$

having $W_{k_p, n_p}^{(j, i)} \simeq W_{k_p, n_{p+1}}^{(j, i)}$ hence

$$\begin{pmatrix} r_{k_p, n_p}^{R, (i)} & -r_{k_p, n_p}^{I, (i, j)} \\ I_{k_p, n_p}^{I, (j)} & r_{k_p, n_p+1}^{R, (j, i)} \end{pmatrix} \begin{pmatrix} W_{k_p, n_p}^{R, (j, i)} \\ W_{k_p, n_p}^{I, (j, i)} \end{pmatrix} = \begin{pmatrix} d_{k_p, n_p}^{(i)} \\ d_{k_p, n_p+1}^{(i)} \end{pmatrix} \quad (10)$$

$$\begin{pmatrix} W_{k_p, n_p}^{R, (j, i)} \\ W_{k_p, n_p}^{I, (j, i)} \end{pmatrix} = \frac{1}{r_{k_p, n_p}^{R, (j)} r_{k_p, n_p+1}^{R, (j)} + r_{k_p, n_p}^{I, (j)} r_{k_p, n_p+1}^{I, (j)}} \times \begin{pmatrix} W_{k_p, n_p}^{R, (j, i)} \\ W_{k_p, n_p}^{I, (j, i)} \end{pmatrix}$$

More compactly

$$W_{k_p, n_p}^{(j, i)} = \frac{d_{k_p, n_p}^{(i)} r_{k_p, n_p+1}^{*(j)} + j d_{k_p, n_p+1}^{(i)} r_{k_p, n_p}^{*(j)}}{\Re(r_{k_p, n_p}^{(j)} r_{k_p, n_p+1}^{*(j)})} \quad (11)$$

We set for each antenna the value of each pair of pilots such that; $d_{k_p, n_p+1}^{(i)} = 0$ and $d_{k_p, n_p}^{(i)} = 1$ with $i \in \{1, \dots, N_t\}$. Thus,

$$W_{k_p, n_p}^{(j, i)} = \frac{r_{k_p, n_p+1}^{*(i)}}{\Re(r_{k_p, n_p}^{(i)} r_{k_p, n_p+1}^{*(i)})} \quad (12)$$

One of the advantages of the *POP* scheme, besides its simplicity is that, it doesn't explicitly depends on the employed prototype filter. However, it must be emphasized that the above derivation only holds when noise is negligible. One can see that in the presence of noise, the method can have unpredictable performance since the degree of the noise enhancement in general also depends on unknown (hence uncontrollable) data.

G. FBMC using scattered pilots

Scattered or orthogonal pilot sequences are usually used to transmit over N_t antennas in CP-OFDM systems [20]. Using such pilot sequences it is possible to recover the channel coefficients for each pair of receive and transmit antennas. As for MIMO CP-OFDM system it is possible to choose the value of the pilot in the form; for instance, $[P_1, P_2]$ for antenna "1", and $[\hat{P}_1, \hat{P}_2]$ for antenna "2" (see references in [20]). The assumption of constant channel over 2 consecutive symbols is fulfilled in OQAM-OFDM (FBMC) system. Adapting the orthogonal pilot sequences to PHYDYAS's FBMC specifications, we start from the equivalent D-PUSC pilot structure for two antennas at the transmitter as depicted in Figure 1, and we propose an adapted pilot structure version for MIMO FBMC as in Figure 8a. Using proposed scattered pilots in Figure 8, with PHYDYAS filter parameters [3] depicted in Table I, we assume that the channel is quasi-static at least over four consecutive FBMC time symbols. As in previous pilot allocation schemes, the main objective is always to cancel the interference caused by the neighboring symbols (see Figure 4). First, orthogonality between the pilot sequences over the antennas could be preserved by setting one of the

pilots to zero. Secondly, the interference is compensated by setting the value of one of the neighbors to the total of the intrinsic interference.

The cancelation of the intrinsic interference is performed in two steps too. First, the $d_{k, n-1}^i$ ($i \in \{1, 2\}$ refers to transmit antenna index) symbol is determined to cancel the interference over (k, n) position. Then $d_{k, n+2}^2$ and $d_{k, n-1}^1$ symbols are determined to cancel the interference over the $(k, n+1)$ and (k, n) respectively. It can be seen in Figure 8, that $d_{k, n+2}^i$ is placed at position $(k, n+2)$, so by modifying the $d_{k, n+2}^i$ value it doesn't generate interference on the symbol located at position (k, n) . As a consequence, this allows to cancel intrinsic FBMC interference in both (k, n) and $(k, n+1)$ time-frequency positions. The values of $d_{k, n}^2$ and $d_{k, n+1}^1$ are here fixed to zero. Note that proposed scattered pilot scheme in Figure 8, could be considered as a special case of the auxiliary pilot scheme depicted in Figure 6.

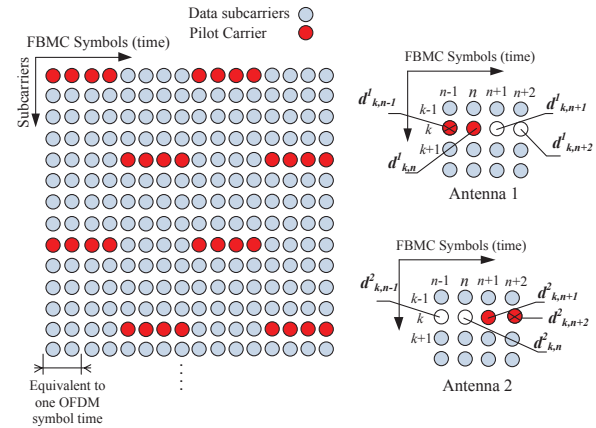


Figure 8. Simplified orthogonal pilot sequences in FBMC MIMO system with 2 transmit antennas: (a) general structure, (b) pilot allocation for each transmitted antenna.

IV. SIMULATIONS RESULTS

The pilot pattern structures were tested using the reference filter bank parameters in PHYDYAS project [2][3], with an overlapping factor $K=4$ and WiMAX-physical layer like basic parameters with: FFT-size and M equal to 1024, a bandwidth of 10 MHz, and subcarrier spacing of 10.94 kHz. This allows a transmission of 53 OQAM symbols. Note that due to the effect of the cyclic prefix in an OFDM based WiMAX system only 47 symbols can be used. During all the simulations the evaluated link is the downlink PUSC (DL-PUSC) structure [11].

In all the simulations received signals are assumed perfectly synchronized in time and frequency domain. The interpolation process is carried out using two dimensional linear surface interpolations within the areas limited by the

carriers and the symbols with pilot supports. Simulations have been run over 600 channel realizations. Note that a weak spatial correlation is assumed for both transmit and receive antennas. The CP-OFDM transmitted signal was again scaled in each experiment so it has to be of the same power with the channel input in the corresponding FBMC/OQAM system. Note that there is no channel coding scheme used during the simulation process.

It can be seen in Figure 9, that the POP scheme adapted for MIMO FBMC exhibited a performance worse than the CP-OFDM schemes for both channels; Veh-A, and Veh-B. A similar strategy for the pair values of $(0, \pm 1)$ for pilots have been adopted as in [19] for each antenna pilot pattern. Although a performance degradation is experienced by the CP-OFDM scheme in the Veh-B channel, the POP scheme still yields worse results in the Veh-A channel. Therefore, it can be concluded that the POP scheme is unsuitable for filter bank multicarrier system due to its poor performance compared with the CP-OFDM scheme.

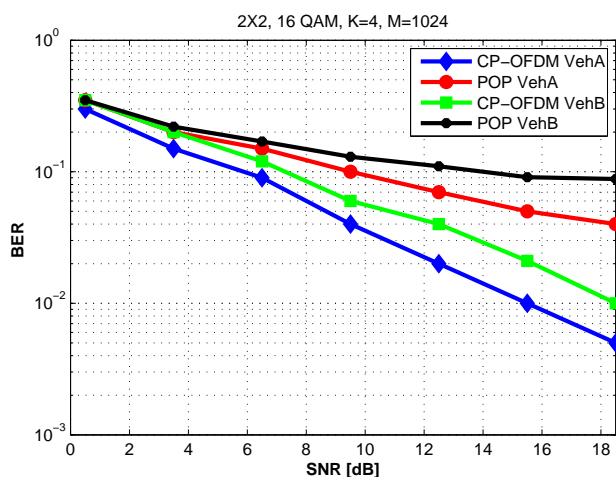


Figure 9. A 2×2 MIMO scheme performances using FBMC and CP-OFDM for Veh-A and Veh-B at 60 Km/h, using adapted POP method to downlink PUSC. Filter bank references: $M=1024$, $K=4$, and 16 QAM modulation with ZF equalization.

In Figure 10 and Figure 11, the use of the two variants of the adapted IAM-R (depicted in Figure 7a, and Figure 7b respectively) are analyzed. In Figure 10, two APC carriers are used to estimate the interference effects of the used filter. Here we dealt with a partial interference approximation as not all the interference $(\Omega_{k_p, n_p} = \Omega_{1,1})$ that affects the pilot d_{k_p, n_p}^i could be estimated. The real values used in $[d_{k_p, n_p-1}^i, d_{k_p, n_p}^i, d_{k_p, n_p+1}^i]$ are $[0, d_{k_p, n_p}^i, 0]$ respectively, with the centered value $d_{k_p, n_p}^i = \pm 1$. It can be also observed that the "IAM-Ra" scheme in Figure (10) performs similarly as the CP-OFDM for SNRs lower than 8 dB for Veh-A channel environment, and for SNRs lower than 5 dB in case of Veh-

B channel environment. An error floor is observed when the IAM is used at high SNRs due to the unavoidable intrinsic interference which is shows up at weak noise regimes.

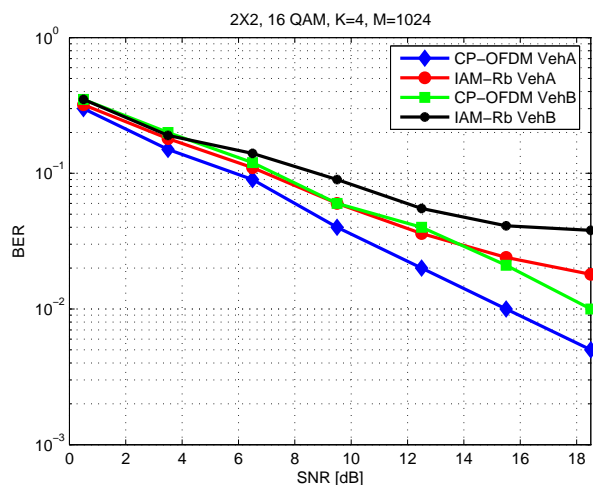


Figure 10. A 2×2 MIMO scheme performances using FBMC and CP-OFDM for Veh-A and Veh-B channels at 60 km/h, using adapted IAM method in DL-PUSC: (a) IAM-Ra refer to scheme in 7a for 2 antennas.

However, a better result is achieved in Figure 11 "IAM-Rb" due to the use of several APC carriers, more exactly four "aided" pilots. In Veh-A channel environment very similar performance in terms of BER is achieved using the FBMC and/or the CP-OFDM scheme. The CP-OFDM performs around 1/2 dB better than the FBMC. In channels with higher frequency selectivity as in Veh-B channel environment, the FBMC system performs similarly as the CP-OFDM up to SNR= 12 dB. For higher values of SNRs the CP-OFDM clearly outperforms the FBMC system. Here the value of d_{k_p, n_p-1}^i , and d_{k_p, n_p+1}^i is zero, and $[d_{k_p-1, n_p}^i, d_{k_p, n_p}^i, d_{k_p+1, n_p}^i]$ use ± 1 values in alternation. The main reason for such alternation is to alleviate the risk of high peaks power [18]. Note that, still not all the interference that affects the pilot d_{k_p, n_p}^i could be estimated but only almost the largest ones.

Figure 12, shows that the use of auxiliary pilots in FBMC system outperforms the conventional CP-OFDM system. In Veh-A channel with 60Km/h of velocity moving the FBMC with Minimum Mean Square Error (MMSE) equalization achieves better performs than the CP-OFDM. Even using the zero forcing (ZF) equalization the performances are lightly better than the CP-OFDM with ZF.

Figure 13, depicts obtained performance with scattered pilots for CP-OFDM and FBMC using non iterative MMSE receiver. It can be observed that for pedestrian channel (type A at 3 km/h of mobility) FBMC performance is very similar to that obtained with a CP-OFDM system. Due to the very

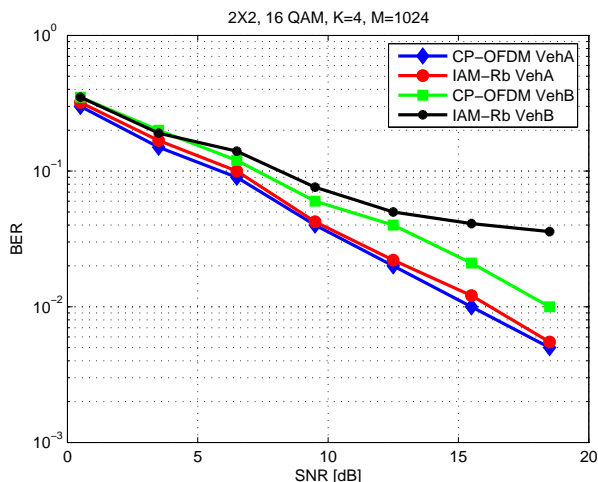


Figure 11. A 2×2 MIMO scheme performances using FBMC and CP-OFDM for Veh-A and Veh-B channels at 60 km/h, using adapted IAM method in DL-PUSC. IAM-Rb (describes scheme in Figure 7b) for 2 antennas. $M=1024$, $K=4$, and 16 QAM with ZF equalization.

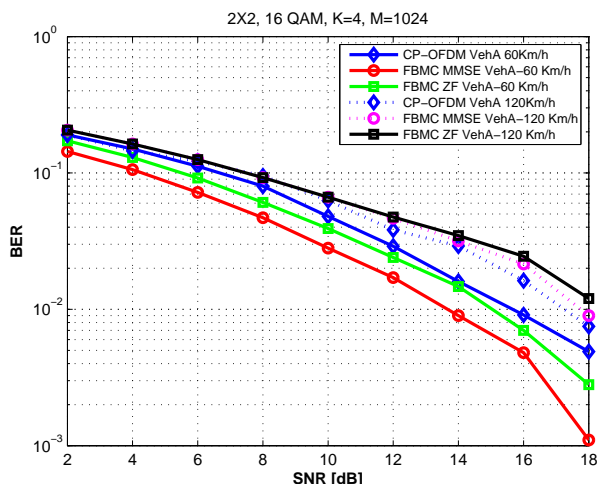


Figure 12. A 2×2 MIMO scheme performances using FBMC and CP-OFDM for Veh-A at different MS velocities (60 Km/h and 120 Km/h), using adapted auxiliary pilot method (see fig. 6) vs. conventional CP-OFDM. $M=1024$, $K=4$, DL-PUSC mode, and 16 QAM using MMSE [17] and ZF equalizations.

low variability of this channel, the assumption of having four FBMC time symbols (equivalent to two OFDM time slots) makes sense as the channel is quasi invariant. In the case of higher frequency selectivity channels, as the Veh-A/B, additional degradation in MIMO can occur in FBMC due the assumption of a constant channel over the symbols besides the interference effect of the first order neighbors.

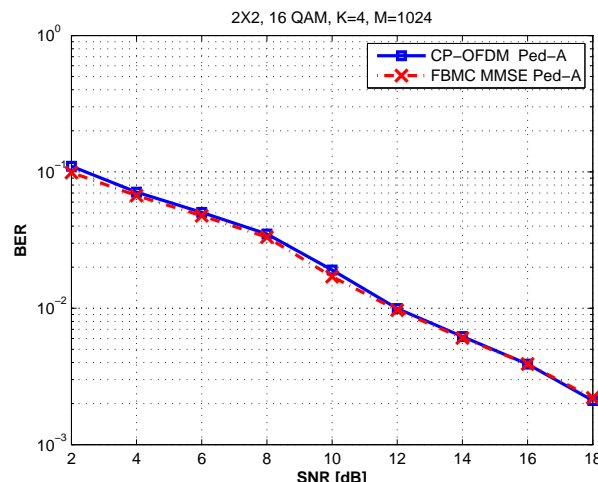


Figure 13. CP-OFDM and FBMC comparison with 2×2 SDM, over Ped-A channel with non iterative MMSE receiver.

V. CONCLUSION

In this paper the authors studied the possibility to adapt the pilot pattern of the DL-PUSC MIMO WiMAX scheme to the MIMO FBMC system. Different scheme have been proposed and their performance evaluated and compared with CP-OFDM system (POP, auxiliary pilot scheme, IAM-Ra, IAM-Rb, and Scattered pilots). Proposed auxiliary pilot scheme seems able to eliminate the secondary interference from the neighboring symbols into the pilots antenna using both the ZF and the MMSE receivers, and to achieve better BER performances than CP-OFDM. Besides, the proposed scheme has the same pilot overhead as in OFDM. The use of scattered pilot for MIMO based on combined auxiliary pilots will be further investigated such that the antennas pilot positions doesn't suffer the effect of the surrounding interference due to the largest weights of the filter banks.

ACKNOWLEDGMENT

The authors would like to thank all the partners of the European ICT 2008-211887 project PHYDYAS.

REFERENCES

- [1] K. Baum, B. Classon, and P. Sartori, "Principles of Broadband OFDM Cellular System Design". Wiley-Blackwell. March 2009.
- [2] ICT-211887 PHYDYAS European project, www.ict-phydyas.org. (visited 31st January 2011).
- [3] ICT-PHYDYAS Deliverable 3.1 "Equalization and demodulation in the receiver (single antenna)", Section: Channel estimation. 2008.
- [4] B. Farhang-Boroujeny, "Filter bank spectrum sensing for cognitive radios," *IEEE Trans. on Signal Processing*, vol. 56, no. 5, pp. 1801-1811. May 2008.

- [5] M. Shaat and F. Bader, "Low Complexity Power Loading Scheme in Cognitive Radio Networks: FBMC Capability", in Proceeding of 20th IEEE International Symposium on Personal, Indoor and Mobile Radio Communications (IEEE PIMRC'2009), pp. 2597-2602. Tokyo, Japan. September 2009.
- [6] B. Farhang-Boroujeny and R. Kempfer, "Multicarrier communication techniques for spectrum sensing and communication in cognitive radios," IEEE Communications Magazine (Special Issue: on Cognitive Radios for Dynamic Spectrum Access), vol. 48, no. 4, pp. 80-85, Apr. 2008.
- [7] H. Zhang, D. L. Ruyet, and M. Terre, "Spectral efficiency analysis in OFDM and OFDM/OQAM based cognitive radio networks," in Proc. of the IEEE Vehicular Technology Conference (IEEE VTC-Spring'09), pp.1-5, Barcelona, Spain. April 2009.
- [8] J. P. Javaudin and D. Lacroix, "Technical description of OFDM/IOTA modulation, 3GPP TSG-RAN-1 meeting no. 31," Tokyo, Japan. Feb 18-21, 2003.
- [9] "Wideband air interface isotropic orthogonal transform algorithm (IOTA) - public safety wideband data standards project - digital radio technical standards TR-8.5 subcommittee," TIA902.BBAB (Physical Layer Specification, March 2003).
- [10] F. Bader and M. Shaat, "Pilot Pattern Adaptation and Channel Estimation in MIMO WIMAX-Like FBMC System," in Proc. of Sixth International Conference on Wireless and Mobile Communications (ICWMC'2010). pp. 111-116. September 2010. Valencia, Spain.
- [11] Part 16: Air Interface for Fixed and Mobile Broadband Wireless Access Systems Amendment 2: Physical and Medium Access Control Layers for Combined Fixed and Mobile Operation in Licensed Bands and Corrigendum 1, IEEE Std. 802.16e, 2006.
- [12] M. Bellanger, "Filter Banks Digital Processing and Signals: Theory and Practice," John Wiley and Sons, New York, NY-USA, 3rd edition 2000.
- [13] M. Bellanger, "Transmit diversity in multicarrier transmission using OQAM modulation," in Proc. of the International Symposium on Wireless Pervasive Computing (ISWPC'2008), Santorini (Greece), May 2008
- [14] M. Bellanger, "Specification and design of a prototype filter for filter bank based multicarrier transmission," Proc. of the IEEE International Conference on Acoustics, Speech, and Signal Processing, (IEEE ICASSP'2001). Vol 4. pp. 2417-2420. Salt Lake City, USA. May 2001.
- [15] R. V. Nee, "OFDM Wireless Multimedia Communications." Artech House. January 2000.
- [16] P. Siohan, C. Siclet, and N. Lacaille, "Analysis and design of OFDM/OQAM systems based on filterbank theory," IEEE Transactions on Signal Processing, vol. 50, no. 5, pp. 1170-1183, 2002.
- [17] J. P. Javaudin and Y. Jiang, "Channel estimation in MIMO OFDM/OQAM," in Proc. of the IEEE International Workshop on Signal Processing Advances for Wireless Communications (IEEE SPAWC'2008). pp. 266-270. Recife, Pernambuco, Brazil, July, 2008.
- [18] C. L  l  , J.-P. Javaudin, R. Legouable, A. Skrzypczak, and P. Siohan, "Channel estimation methods for preamble-based OFDM/OQAM modulations," European Transactions on Telecommunications (ETT), Vol 19, Issue 7, pp. 741-750. November 2008.
- [19] J. P. Javaudin, D. Lacroix, and A. Rouxel, "Pilot-aided channel estimation for OFDM/OQAM," in Proc. of the IEEE Vehicular Technology Conference (VTC-spring 2003), pp. 1581-1585, April 2003.
- [20] N. Chen, M. Tanaka, and R. Heaton, "Channel Equalisation for OFDM using scattered pilots," in Proc. of the IEEE Vehicular Technology Conference (IEEE VTC-Spring'2002). pp. 1040-1044. Birmingham, Alabama-USA. May 2002.